COMPUTER-ASSISTED ANALYSIS OF FOURIER TRANSFORM INFRARED (FTIR) SPECTRA FOR CHARACTERIZATION OF VARIOUS TREATED AND UNTREATED AGRICULTURE BIOMASS

Siong Fong Sim,* Murtedza Mohamed, Nurul Aida Lu Mohd Irwan Lu, Noor Safitri P. Sarman, and Siti Nor Sihariddh Samsudin

A computational approach was used to analyze the FTIR spectra of a wide range of treated and untreated lignocellulosic biomass (coconut husk, banana trunk, sago hampas, rice husk, and empty fruit bunch). The biomass was treated with strong sulphuric acid and NaOH, respectively. A total of 87 spectra were obtained in which the absorption bands were de-convoluted automatically, generating a peak table of 87 rows and 60 columns. Square roots were taken of the peak values, with further standardization prior to Principal Component Analysis (PCA) for data exploration. In a scores plot, the treated and untreated biomass were distinguishable along the two main axes, PC1 and PC2. Examining the absorption bands corresponding to lignocellulosic components indicated that the acid pretreatment had resulted in dissolution and degradation of hemicelluloses and lignin, confirmed typically by disappearance of bands. The alkali treatment however was not as rigorous as the acid treatment, as some characteristic bands of hemicelluloses and lignin were enhanced, suggesting condensation of the degraded polysaccharides. The computer-assisted analysis of the FTIR spectra allowed efficient and simultaneous comparisons of lignocellulosic compositions present in various treated and untreated biomass. This represents an improvement relative to the conventional methods, since a large dataset can be handled efficiently and individual peaks can be examined.

Keywords: Lignocellulosic biomass; Fourier Transform Infrared; Peak detection and matching; Principal Component Analysis (PCA)

*Contact information: Universiti Malaysia Sarawak, Faculty of Resource Science and Technology, 94300 Kota Samarahan, Sarawak, Malaysia; *Corresponding author: sfsim@frst.unimas.my*

INTRODUCTION

Fourier Transform Infrared (FTIR) spectroscopy is commonly used to study the functional groups of lignocellulosic biomass and the changes caused due to different treatments. The spectra offer qualitative and semi-quantitative information suggesting the presence and absence of lignocellulosic compounds, and whether the intensity of an absorption band has changed after treatment (Li *et al.* 2010). This technique is well known for its simplicity in sample preparation and speed of analysis (Davis and Mauer 2010). One could easily generate hundreds of spectra within a short period of time. However, the process of spectral integration could turn out to be complicated and tedious. For this reason, the application of FTIR for lignocellulosic studies typically involves

spectral comparisons of 1 to 3 biomass species with a limited number of samples (Davis and Mauer 2010; Daffalla *et al.* 2010; Ding *et al.* 2012). Very often, the analyst overlays the spectra for visual interpretation; however when there are too many spectra, such an approach is unlikely to yield comprehensible information. In this paper, we incorporated a computational approach to examine the FTIR spectra of 15 biomass species, including 5 raw biomass types, each treated with acid and alkali, respectively. Fundamentally, the absorption bands were de-convoluted automatically, generating a peak table readily available for multivariate analysis. In addition, it allowed straightforward and efficient comparisons across various lignocellulosic biomass. We focused on Principal Component Analysis (PCA) of the peak table, limiting attention to the two most prominent components, PC1 and PC2. Bands corresponding primarily to cellulose, hemicelluloses, and lignin were considered to identify changes due to different treatments. The observations attained were confirmed with the literature references.

The peak detection algorithm has been reported for analysis of edible oils (Sim and Ting 2012). In fact, this approach has been widely applied for various applications including GC-MS (Dixon *et al.* 2007), LC-MS (Zhang and Haskins 2010; Frederiksson *et al.* 2009), GC-GC (Peters *et al.* 2007), GC-DMS (Sim *et al.* 2010), and NMR (Van and Shaka 1998). The computational approach is not perfect; for instance, it may introduce falsification such as mismatching of peaks. Nevertheless it is an alternative to examine a large dataset systematically with promising efficiency (Dixon *et al.* 2007; Sim *et al.* 2010; Frederiksson *et al.* 2009).

The algorithm allows users to adjust several parameters to produce an optimal peak table *i.e.*, peak noise factor, peak filtering window, and peak matching window. The peak noise factor is used to determine the potential signal threshold. If the peak noise factor is too low, then background noise will be identified as peaks, whilst a large value will cause peaks to be missed. The peak filtering window rejects peaks with small width, whereas the peak matching window decides whether peaks found in different samples are to be assigned to the same functional groups. If a window of ± 5 scans is set, peaks at 1702 and 1706 cm^{-1}, found in two different samples, will be assigned to the same functional group. However, if two characteristic peaks at 1702 and 1710 cm^{-1} are anticipated to represent the same functional group but have been identified as two different peaks in the peak table, such a situation suggests that the peak matching window is not suitable. The parameters are often set according to users' experience. In general it is recommended to evaluate the peak table using various settings as suggested in Sim and Ting 2012. In this paper, the peak detection and matching parameters were set as follows: peak noise factor (5); peak filtering window (10 scans); and peak matching window (± 10 scans).

EXPERIMENTAL

Sample Preparation

The agriculture biomass selected included coconut (*Cocos nucifera*) husk, banana (*Musa cavendish*) trunk, sago (*Metroxylon sagu*) hampas, rice (*Oryza sativa*) husk, and oil palm (*Elaeis guineensis*) empty fruit bunches. The biomass was provided by local

industries. They were washed extensively with running tap water to remove dirt and cut into smaller pieces (1 to 2 cm). They were then oven dried at 105 °C for 24 hrs, ground with a grinder, and stored in desiccators. The mesh size of the ground biomass was less than 300 µm.

Treatment Processes

The ground biomass was treated with acid and alkali, respectively, according to Fernando *et al.* 2009. For acid pretreatment, the ground biomass was mixed with 97% concentrated sulfuric acid (H_2SO_4) in a 1:1 ratio, and placed in an oven at 200 °C for 24 h. The samples were allowed to cool to room temperature, washed with distilled water, and soaked in 1% $NaHCO_3$ solution for 1 hr to remove the remaining acid. The samples were then washed with distilled water, and the pH was adjusted to 6.5 with a 1% sodium bicarbonate solution ($NaHCO_3$). The samples were placed in an oven at 105 °C for 24 hrs and were stored in airtight containers.

For alkali pretreatment, the ground biomass was mixed with 0.25 M of sodium hydroxide (NaOH) in a 1:10 ratio and left for 1 hr. The samples were neutralized with hydrochloric acid (HCl) and washed thoroughly with distilled water. The washed materials were dried at 105 °C in an oven for 24 hrs. The products were stored in airtight containers.

Infrared Spectroscopic Studies

The functional groups were characterized with FTIR. All spectra were obtained on a Perkin Elmer FTIR system using the potassium bromide (KBr) disc method with a 2 mg of sample (± 0.2 mg) in 100 mg KBr. Note that it is important to maintain the ratio of sample against KBr so that the lignocellulosic fractions of different biomass are comparable. Six replicates were scanned for each biomass from 4000 to 400 cm^{-1} at a resolution of 4 cm^{-1} to demonstrate the repeatability of the spectral response.

Data Analysis

A total of 87 spectra of untreated and treated biomass were acquired, of which 29 were raw biomass, 28 were acid-treated, and 30 were alkali-treated samples. Prior to analysis, the spectra were overlaid for inspection; some atypical spectra were excluded. The computational approach was used to find peaks and match them automatically producing a peak table for multivariate analysis (Sim and Ting 2012). In addition, the peak table can be used to determine the quantitative and qualitative variation of various biomass. If a peak is commonly found in replicates of a biomass species, this confirms the presence of the peak. Similarly, if a peak is consistently more abundant, it validates the predominating nature of the peak in the biomass.

The analysis involved the conversion of FTIR spectra in SP format to Matlab. Each spectrum was a vector of dimensions (3601 × 1) with a resolution of 1 cm^{-1}. The spectrum was baseline corrected, where a Whittaker smoother was used to estimate the baseline and the signal was corrected using the asymmetric least squares approach (Boelens *et al.* 2004).

The baseline-corrected spectra were subjected to the peak detection and matching algorithm (Sim and Ting 2012). The algorithm is not described for brevity. Briefly, the

algorithm de-convoluted the spectrum into the first derivative signal, where the peak start, peak, and peak end were determined. The algorithm recorded the peaks present in each spectrum, including where they were found and the corresponding peak areas. The peak area was calculated as the sum of the detector output from the peak start to the peak end. The peaks identified in each spectrum were matched across samples, and peaks found in a series of spectra with similar frequencies were assigned to the same functional group, yielding a peak table with rows corresponding to samples and columns to variables (in wavenumber/ (cm^{-1})).

If a peak was detected in a sample, it was represented by its peak area on the peak table; otherwise zeros were entered in the table. Subsequent to the peak detection and matching process, variables that were present inconsistently and detected in less than five samples were eliminated, as they were regarded as possibly noise.

Multivariate Analysis

The algorithm produced a peak table of dimensions (87 × 60). The peak table was preprocessed by taking the square-roots of the values to reduce the influence of variables with large peak area, and the columns of the data matrix were standardized to ensure each variable had a similar influence. The preprocessed peak table was subjected to Principal Component Analysis (PCA).

PCA was used to establish the underlying grouping structures of various biomasses. The correlated variables of multivariate data were transformed to a number of uncorrelated variables called Principal Components (PCs). PCA is performed using the non-linear iterative partial least squares (NIPALS) algorithm in which the data are decomposed into scores, ***T*** and loadings, ***P*** (Esbensen 1998).

RESULTS AND DISCUSSION

The FTIR spectra of various untreated and treated biomass are shown in Fig. 1. Different biomass were hardly distinguishable by visual inspection. Nevertheless, the treated biomass samples clearly exhibited increased intensities in the regions of 3400 cm^{-1}, 1700-1500 cm^{-1}, and 1200-1000 cm^{-1}.

The algorithms report several absorption bands commonly found in biomass at 1157 cm^{-1}, 1329 cm^{-1}, 1370 cm^{-1}, 1423 cm^{-1}, and 2923 cm^{-1}. The peak assignments are summarized in Table 1. These absorption bands are associated with the presence of lignocellulosic components, *i.e.*, cellulose, hemicelluloses, and lignin. Fundamentally, cellulose is formed by glycosidic linkages and hydroxyl groups with a small amount of carboxyl, whilst hemicellulose and lignin are predominated by ether bonds with hemicellulose characterized by a significant amount of carboxyl groups (Taherzadeh and Karimi 2008). The common glycosidic linkages explain the presence of the absorption band at 1157 cm^{-1} in all untreated biomass, attributable to C-O-C ring vibrational stretching.

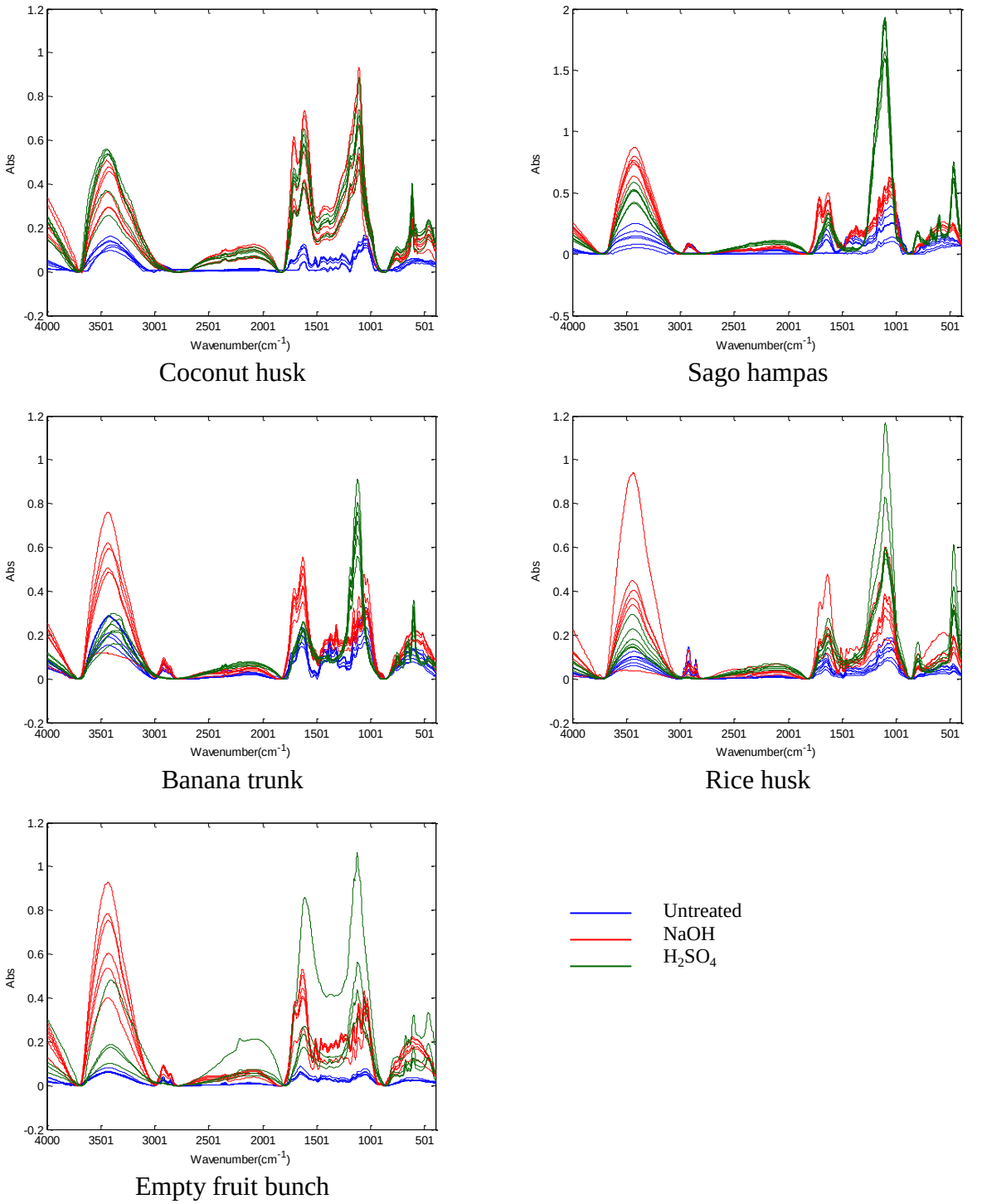

Fig. 1. FTIR spectra of various treated and untreated biomass according to species

Table 1. Absorption Peaks Detected and the Corresponding Functional Groups

Wavenumber, cm^{-1}	Functional groups
1031	C-O, C=C, C-C-O vibrational stretching (Ding *et al.* 2012)
1043	C-O, C-C and C-OH stretching vibrations of cellulose, hemicelluloses and lignin (Ding *et al.* 2012; Shi and Li 2012)
1060	C-OH stretching vibration of the cellulose and hemicelluloses (Bessadok *et al.* 2007; Shi and Li 2012)
1157	C-O-C ring vibrational stretching of β(1,4)-glycosidic linkage for cellulose I and cellulose II (Zhou *et al.* 2009; Shi and Li 2012)
1266	Syringyl ring breathing and C-O stretching in lignin and xylan (Shi and Li 2012)
1319	C-H in plane bending of cellulose I and cellulose II (Shi and Li 2012)
1370	Aliphatic C-H stretching in methyl and phenol alcohol (Shi and Li 2012)
1427	Aromatic skeletal combined with C-H in plane deforming and stretching (Shi and Li 2012)
1457	The aliphatic part of lignin (Shi and Li 2012)
1511	C=C stretching vibrations of the aromatic rings of lignin (Ghali *et al.* 2012)
1640	C=O stretching vibration in conjugated carbonyl of lignin (Shi and Li 2012)
1730	C=O stretching of hemicellulose (Ghali *et al.* 2012)
2855, 2890, 2923	C-H stretching of lignocellulosic components (Ding *et al.* 2012)
3392, 3412 (broad)	Hydrogen bonded OH bond stretching vibration of α-cellulose (Ghali *et al.* 2012)

The preprocessed peak table was subjected to PCA yielding scores (***T***) and loadings (***P***) to describe the underlying relationships between samples and variables. Figure 2 shows the scores plots of PC 2 against PC 1, where the samples are labeled according to biomass; the blue, red, and green markers denote untreated, alkali- and acid-treated samples, respectively. The scores plot suggests that the treated and untreated biomass are distinguishable as respective groups of samples clustered accordingly. However, alkali-treated coconut husk appeared to group within the acid-treated samples. This suggests that NaOH-treated coconut husk may share similar functional group properties as those of the acid-treated samples, specifically along PC1 and PC2, which explain 65% of the spectral variation. For each cluster corresponding to different treatments, the scores plot did not demonstrate a well-defined separation between biomass. The data points were overlapped considerably; however it was possible to extract samples of interest from the overall peak table of (87 × 60) yielding a reduced peak table for PCA.

Figure 3 illustrates the scores plots generated with the reduced peak tables of untreated and treated biomass, respectively. The scores plots indicate that samples could possibly be separated according to biomass species according to treatments. Figure 4 illustrates the loadings plot attained using the overall peak table. The data points over-lapped, rendering the interpretation process challenging and uninformative. However it is

possible to subject the peak table to variable selection to determine the discriminatory variables, as demonstrated elsewhere (Sim and Ting 2012). In this study, we focused on investigating the designated lignocellulosic bands.

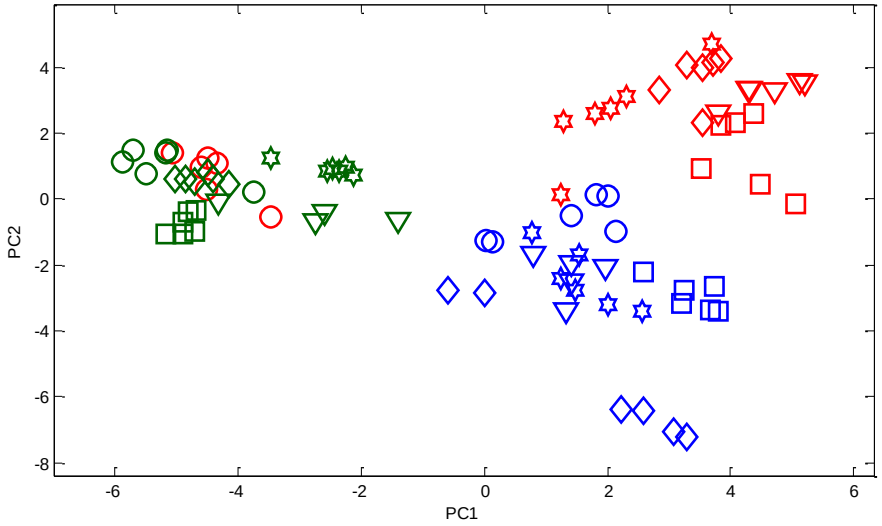

Fig. 2. PCA scores plot according to agricultural biomass based on the peak table

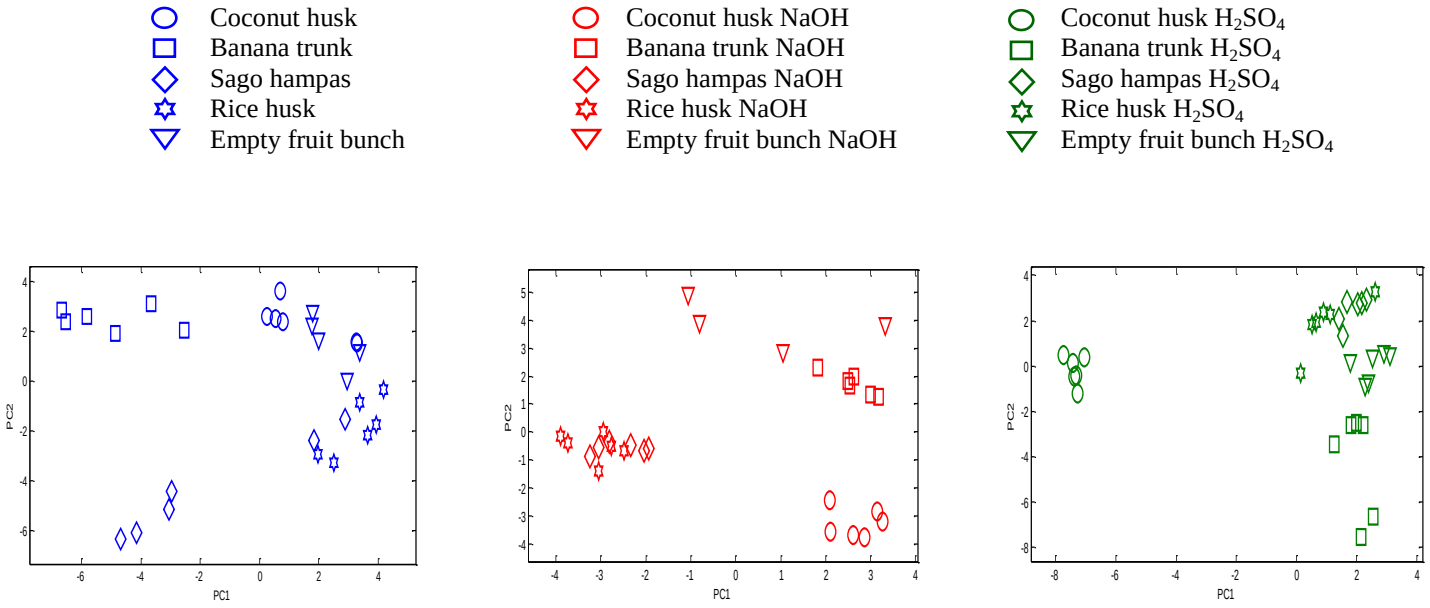

Fig. 3. PCA scores plots according to treatments based on the reduced peak table

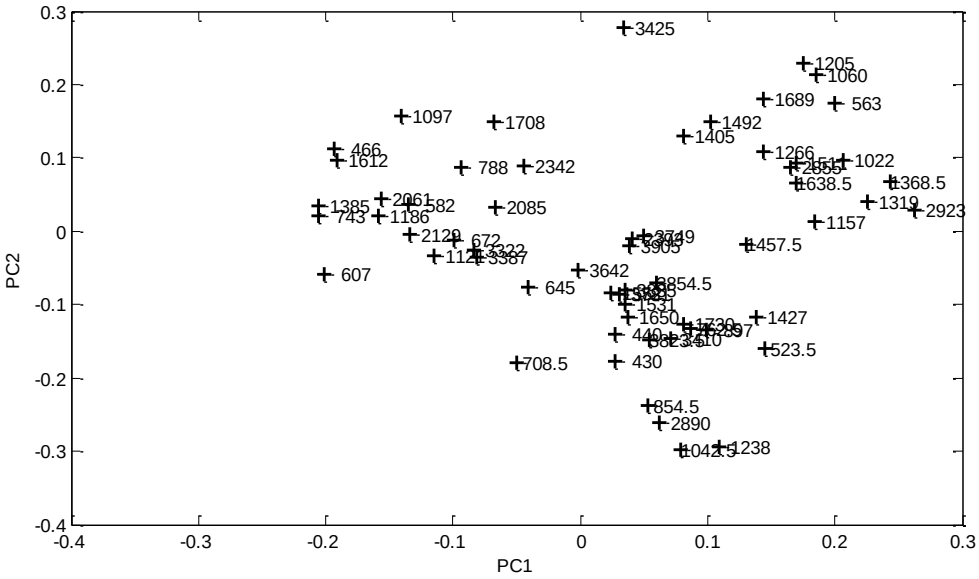

Fig. 4. Loadings plot according to the peak table involving all samples based on the peak table

Figure 5 illustrates the relative abundance of various lignocellulosic bands in the untreated biomass. The spectral region on the right verifies the abundance of the absorption bands reported in the peak table. The absorption bands at 1157 cm^{-1} and 1319 cm^{-1}, characteristic of hemicelluloses and cellulose, are relatively more abundant in sago hampas and banana trunk suggesting that they are richer in cellulose and hemicelluloses constituents. The observations corroborated the lignocellulosic compositions reported elsewhere: sago hampas (64.4% cellulose; 25.1% hemicellulose; 10.5% lignin), banana trunk (63 to 64% cellulose; 19% hemicellulose; 5% lignin), coconut husk (39.31% cellulose; 16.15% hemicellulose; 29.79% lignin), rice husk (25 to 35% cellulose; 18 to 21% hemicellulose; 26 to 31% lignin), oil palm fruit bunch (44.2% cellulose, 33.5% hemicellulose; 20.4% lignin) (Kuroda *et al.* 2001; Taj *et al.* 2007, Luduena *et al.* 2011; Vaithanomsat *et al.* 2011; Azis *et al.* 2002).

The absorption band at 1511 cm^{-1}, which is indicative of the aromatic characteristic of lignin, is found in almost all untreated biomass, where a higher abundance is observed in coconut husk as reported in Hernandez *et al.* 2007. In sago hampas, a shoulder band is exhibited; however it is too weak to be identified as a peak, suggesting the low lignin content. The algorithm can be tuned accordingly to investigate a specific peak shift by reducing the peak matching window. For example, Corredor *et al.* 2009 revealed that the lignin band in softwood is shifted to a higher wavenumber (> 1511 cm^{-1}). In the present study, the algorithm identified the absorption band at 1511 cm^{-1} in coconut husk and empty fruit bunch; however the band is shifted to 1515 cm^{-1} in rice husk and banana trunk. The observation has no relevance to the wood origin, since the two species are neither hardwood nor softwood, but the results may be attributed to differences in the lignin.

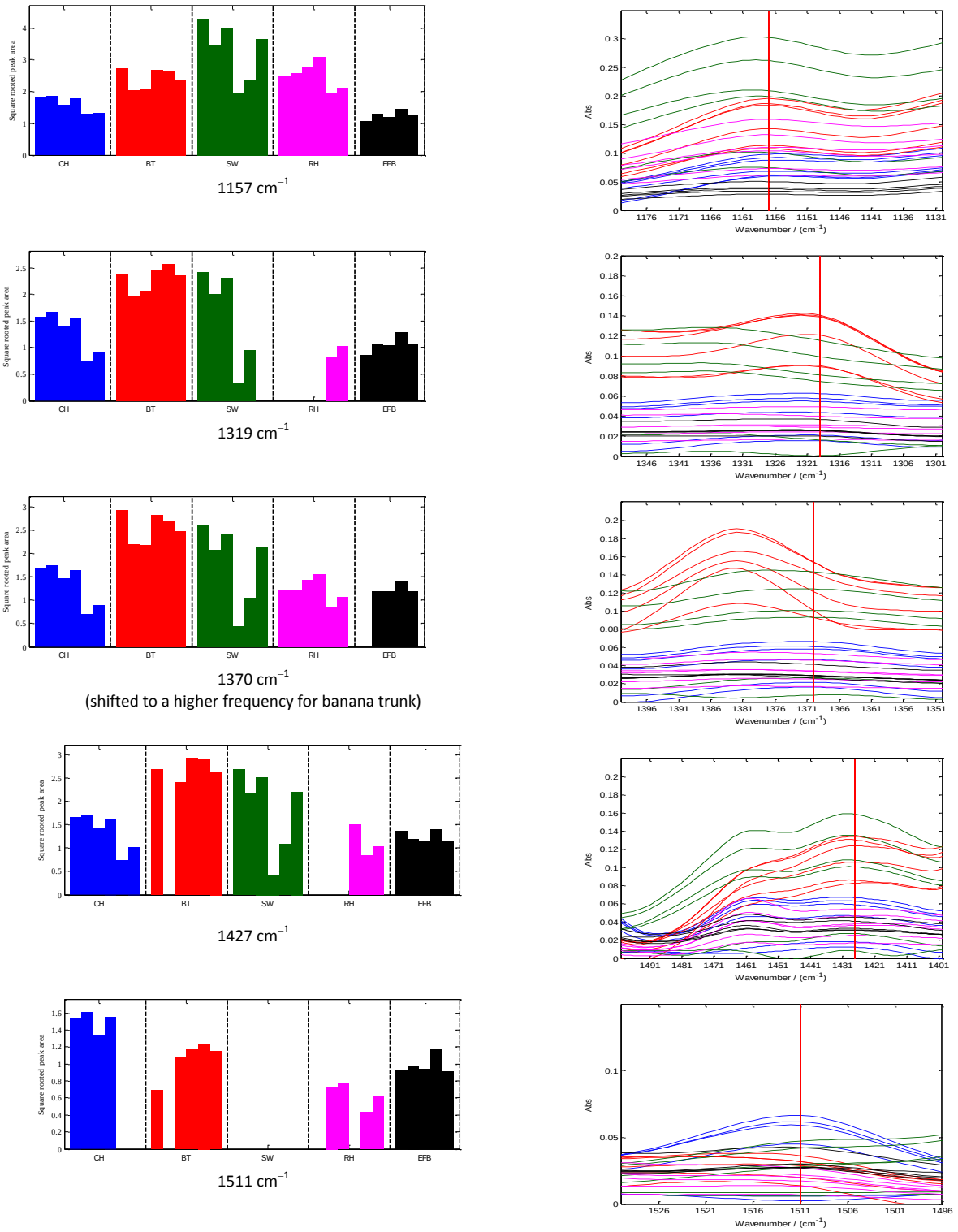

Fig. 5. The bar charts illustrating the relative abundance of some important lignocellulosic components in raw biomass and the corresponding spectral region

Numerous absorption bands are possibly associated with hemicelluloses due to the vast structural diversity *i.e*., 1462, 1419, 1384, 1330, 1244, 1162, 1122, 1090, 1040, 986, and 897 cm^{-1} (Peng *et al.* 2009). The intensity changes at 1157 cm^{-1} had been used to reflect the contribution of hemicelluloses with arabinosyl residues (Kačuráková *et al.* 2000). In Fig. 5, the relative abundance of 1157 cm^{-1} suggests that hemicelluloses of this group are more prominent in sago hampas. Similarly, the typical absorption band of α-glucan at 1042 cm^{-1}, common components of hemicelluloses, is found prevailing in sago hampas. Nevertheless the absorption band at 1064 cm^{-1}, suggested as glucomannan (Kačuráková *et al.* 2000), is identified distinctively in coconut husk and rice husk. This implies that different biomass is characterized by different hemicelluloses components.

Figure 6 shows the bar charts illustrating the relative abundance of some lignocellulosic bands before and after treatments. Fundamentally, acid and alkali pretreatments are employed to remove lignin and hemicelluloses; the spectral changes often involve variation in the band intensity. In this study one can observe the disappearance of typical hemicelluloses and lignin bands at 1157, 1267, and 1511 cm^{-1}. This observation corroborates the findings of Jabasingh and Nachiyar (2012); nevertheless, in some alkali treated biomass, the bands are conversely enhanced. The increased band intensity after treatment is similarly reported in Samuel *et al.* 2011 and Kristensen *et al.* 2008. It is suggested that the increases occur as a result of accumulation of condensed degraded polysaccharides and breakage of lignin, which transforms the original three-dimensional network structure to a linear structure (He *et al.* 2008). Li *et al.* (2010) in addition revealed diminished band intensities at 1056, 1235, and 1375 cm^{-1} after treatment. These bands are generally absent after strong acid treatment but remain in alkali treated samples, suggesting that the acid treatment leads to a greater extent of delignification and dissolution of hemicelluloses. The changes observed also indicate that biomass species are susceptible to treatment in varying degrees. As illustrated in Fig. 6, hemicelluloses and lignin of coconut husk are effectively removed under mild alkali condition, confirmed by the disappearance of bands. This, however, is not evidenced in other alkali-treated biomass; for this reason, the alkali treated coconut husk appears to resemble the acid-treated biomass, clustering within the acid-treated samples (as illustrated in the scores plot in Fig. 2). Other changes include the disappearance of C-H stretching band at 2923 cm^{-1}, signifying a reduction in aliphatic fraction of waxes (He *et al.* 2008; Kristensen *et al.* 2008). Meanwhile, the absorption bands at 1097 and 895 cm^{-1} can be monitored to investigate the crystalline and amorphous cellulose, respectively (Corredor 2008). The band at 1097 cm^{-1} is well defined after treatment, indicating exposure of cellulose; however it is completely missing in acid-treated banana trunk and empty fruit bunch implying degradation of cellulose. The amorphous band, on the other hand, is genuinely weak in most biomass except banana trunk and empty fruit bunch. After pretreatment, the band likewise disappeared, confirming the degradation of amorphous cellulose. Generally, the strong acid pretreatment resulted in the disappearance of most lignocellulosic bands, while retaining several strong absorption bands in the regions of 800-500, 1200-1000, and 1620-1600 cm^{-1}.

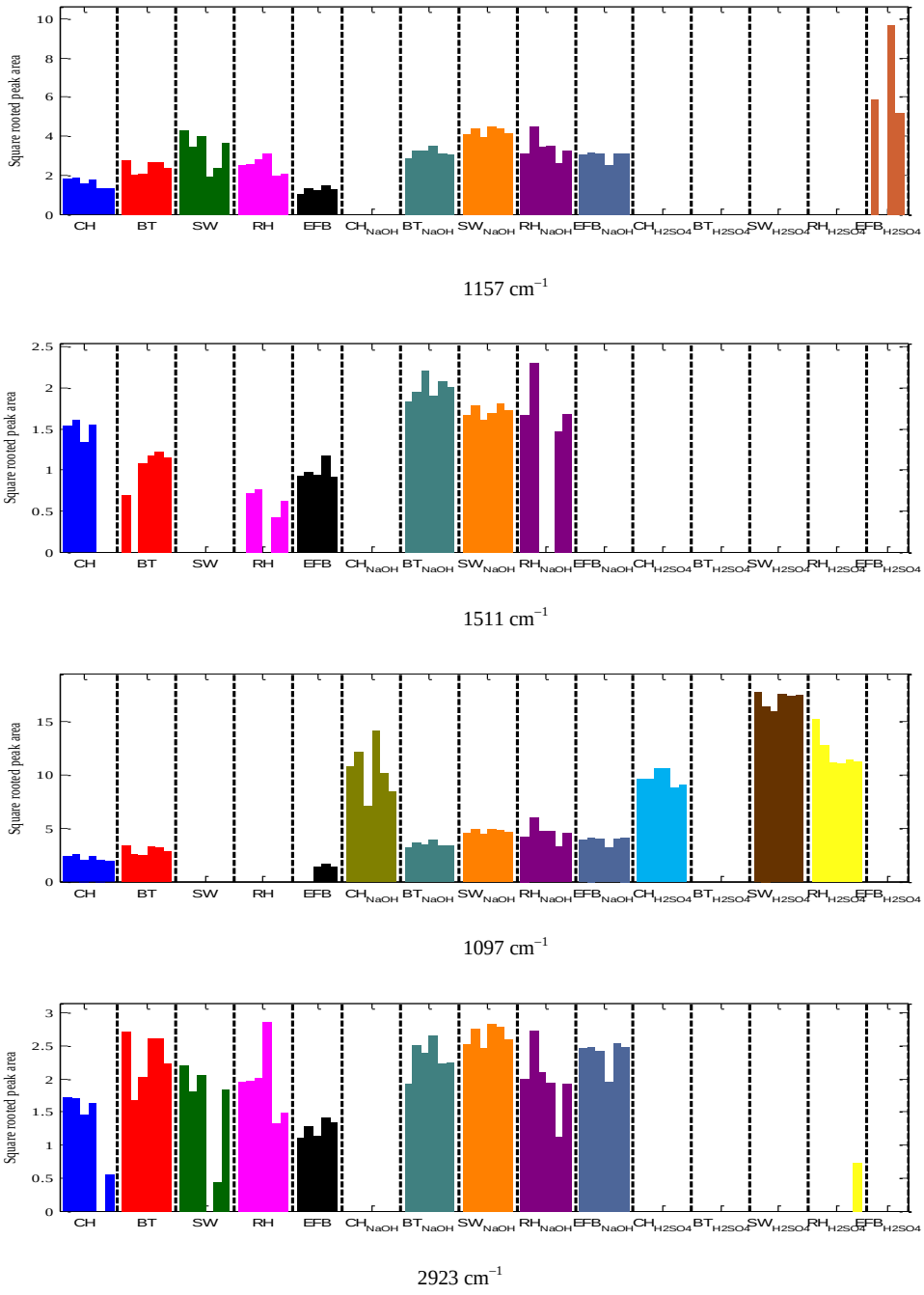

Fig. 6. Bar charts illustrating the relative abundance of some important lignocellulosic components in treated and untreated biomass

Conventionally, the FTIR spectra of lignocellulosic biomass are examined manually; this approach is infeasible when a large number of spectra are involved. Alternatively, the entire signal can be combined, yielding a matrix for PCA to reveal the underlying pattern of the data. However, individual peaks are unable to be located and examined directly with this approach. The computational approach offers an

improvement to the conventional analysis, where the scores plot obtained with the peak table exhibits a comparable pattern to that of the combined spectra (figure not shown). This suggests the feasibility of the computational approach. In addition, individual peaks can be examined separately. Nevertheless, one is required to optimize the peak table with suitable parameters. This involves evaluation of various settings and careful interpretation of the peak table before it is finalized.

CONCLUSIONS

1. As a whole, agriculture biomass samples are primarily characterized by the presence of lignocellulosic components with diverse compositions.
2. The lignocellulosic components are biopolymers having extensive structural diversity; the analysis can become very complicated as the data size increases. The computational approach is incorporated to provide reliable information on the lignocellulosic compounds and to study the changes caused due to different treatments.
3. Acid and alkali pretreatments were shown to have resulted in degradation and dissolution of lignin and hemicelluloses to a different extent. Acid pretreatment is generally more rigorous than the alkali pretreatment, as various absorption bands due to lignin and hemicelluloses are removed after treatment.
4. The information derived allows rapid monitoring of the lignocellulosic compositions in numerous biomass samples.

ACKNOWLEDGMENTS

The authors are grateful for the support of The Ministry of Science and Technology (MOSTI), Grant. No. 06-01-09-SF0086. The authors also thank Dr. Awang Ahmad Sallehin and Dole Sebiro for providing the biomass samples.

REFERENCES CITED

Azis, A.A., Husin, M., and Mokhtar, A. (2002). "Preparation of cellulose from oil palm empty fruit bunches via ethanol digestion: Effects of acid and alkali catalysts," *J. Oil Palm Res.*, 14, 9-14.

Bessadok, A., Marais, S., Gouanve, F., Colasse, L., Roudesli, S., Zimmerlin, I., and Metayer, M. (2007). "Effect of chemical treatments of Alfa (*Stipa tenacissima*) fibres on water-sorption properties," *Compo. Sci. Technol.* 67, 685-697.

Boelens, H. F. M., Dijkstra, R. J., Eilers, P. H. C., Fitzpatrick, F., and Westerhuis, J. A. (2004). "New background correction method for liquid chromatography with diode

array detection, infrared spectroscopic detection and Raman spectroscopic detection," *J. Chromatogr. A* 1057(1-2), 21-30.

Corredor, D.Y. (2008). "Pretreatment and enzymatic hydrolysis of lignocellulosic biomass," *PhD Dissertation*, Kansas State University, Manhattan.

Corredor, D.Y., Salazar, J.M., Hohn, K.L., Bean, S., Bean, B., and Wang, D. (2009). "Evaluation and characterization of forage Sorghum as feedstock for fermentable sugar production," *Appl. Biochem. Biotechnol.* 158(1), 164-179.

Daffalla, S. B., Mukhtar, H., and Shaharun, M. S. (2010). "Characterisation of adsorbent developed from rice husk: Effect of functional group on phenol adsorption," *J. Appl. Sci.* 10(12), 1060-1067.

Davis, R., and Mauer, L. J. (2010). "Current research, technology and education topics in applied microbiology and microbial biotechnology," Formatex, Badajoz.

Ding, T. Y., Hii, S. L., and Ong, L. G. A. (2012). "Comparison of pretreatment strategies for conversion of coconut husk fiber to fermentable sugars," *BioResources* 7(2), 1540-1547.

Dixon, S. J., Brereton, R. G., Soini, H. A., Novotny, M. V., and Penn, D. J. (2007). "An automated method for peak detection and matching in large gas chromatography-mass spectrometry datasets," *J. Chemometr.* 20(8-10), 325-340.

Esbensen, K. (1998) *Multivariate Analysis in Practice*, Third Ed., CAMO, Oslo.

Fernando, A., Monteiro, S., Pinto, F., and Mendes, B. (2009). "Production of biosorbents from waste olive cake and its characteristics for Zn^{2+} ion," *Sustainability* 1(2), 277-297.

Frederiksson, M. J., Petersson, P., Axelsson, B. O., and Bylund, D. (2009) "An automated peak finding method for LC-MS data using Gaussian second derivative filtering," *J. Sep. Sci.* 32(22), 3906-3918.

Ghali, A. E., Marzoug, I. B., Baouab, M. H. V., and Roudesli, M. S. (2012). "Separation and characterization of new cellulosic fibres from the *Juncus acutus* plant," *BioResources* 7(2), 2002-2018.

He, Y., Pang, Y., Liu, Y., Li, X., and Wang, K. (2008). "Physicochemical characterization of rice straw pretreated with sodium hydroxide in the solid state for enhancing biogass production," *Energy Fuels* 22(4), 2775-2781.

Hernandez, J. R., Capareda, S. C., and Aquino, F. L. (2007). "Activated carbon production from pyrolysis and steam activation of cotton gin trash," in: *Proceedings of the Beltwide Cotton Conferences*, Jan 9-12, New Orleans.

Jabasingh, S. A., and Nachiyar, C. V. (2012). "Optimization of cellulase synthesis by RSM and evaluation of ethanol production from enzymatically hydrolysed sugarcane bagasse using *Saccharomyces cerevisiae*," *J. Sci. Ind. Res.* 71, 353-359.

Kačuráková, M., Capek, P., Sasinková, V., Wellner, N., and Ebringerová, A. (2000). "FT-IR study of plant cell wall model compounds: Pectin polysaccharides and hemicelluloses," *Carbohyd. Polym.* 43(2), 195-203.

Kristensen, J. B., Thygesen, L. G., Felby, C., Jørgensen, H., and Elder, T. (2008). "Cell-wall structural changes in wheat straw pretreated for bioethanol production," *Biotechnol. Biofuels* 1(5), 1-9.

Kuroda, K., Ozawa, T., and Ueno, T. (2001). "Characterization of sago palm (*Metroxylon sagu*) lignin by analytical pyrolysis," *J. Agric. Food Chem.* 49, 1840-1847.

Li, C., Knierim, B., Manisseri, C., Arora, R., Scheller, H. V., Auer, M., Vogel, K. P., Simmons, B. A., and Singh, S. (2010). "Comparison of dilute acid and ionic liquid of switchgrass: Biomass recalcitrance, delignification and enzymatic saccharification," *Bioresource Technol.* 101(13), 4900-4906.

Luduena, L., Fasce, D., Alvarex, V.A., and Stefani, P.M. (2011) "Nanocellulose from rice husk following alkaline treatment to remove silica," *BioResources* 6(2), 1440-1453.

Peng, F., Ren, J. L., Bian, J., Peng, P., and Sun, R. C. (2009). "Comparative study of hemicelluloses obtained by graded ethanol precipitation from sugarcane bagasse," *J. Agric. Food Chem.* 57, 6305-6317.

Peters, S., Vivó-Truyols, G., Marriott, P., and Schoenmakers, P. (2007) "Development of an algorithm for peak detection in comprehensive two-dimensional chromatography," *J. Chrom. A* 1156 (1-2), 14-24.

Samuel, R., Foston, M., Jiang, N., Allison, L., and Ragauskas, A. J. (2011). "Structural changes in switchgrass lignin and hemicelluloses during pretreatments by NMR analysis," *Polym. Degrad. Stabil.* 96(11), 2002-2009.

Shi, J., and Li, J. (2012). "Metabolites and chemical group changes in the wood forming tissue of *Pinus koraiensis* under inclined condition," *BioResources* 7(3), 3463-3475.

Sim, S. F., and Ting, W. (2012). "An automated approach for analysis of Fourier Transform Infrared Spectra (FTIR) of edible oils," *Talanta* 88, 537-543.

Sim, S. F., Rearden, P., Kanchagar, C., Sassetti, C., Trevejo, J., and Brereton, R. G. (2010). "Automated peak detection and matching algorithm for gas chromatography-differential mobility spectrometry," *Anal. Chem.* 83, 1537-1546.

Taherzadeh, M. H., and Karimi, K. (2008). "Pretreatment of lignocellulosic wastes to improve ethanol and biogas production: A review," *Int. J. Mol. Sci.* 9, 1621-1651.

Taj, S., Munawar, A. M., and Khan, S. (2007). "Natural fiber-reinforced polymer composites." *Proc. Pakistan Acad. Sci.* 44(2), 129-144.

Vaithanomsat, P., Apiwatanapiwat, W., Chumchuent, N., Kongtud, and Sundharajun, S. (2011). "The potential of coconut husk utilization for bioethanol production," *Kasetsart J. Nat. Sci.* 45, 159-164.

Van, Q. N., and Shaka, A. J. (1998) "Improved cross peak detection in two-dimensional proton NMR spectra using excitation sculpting," *J. Magn. Reson.* 132, 154-158.

Zhang, J. Q., and Haskins, W. (2010). "ICPD – A new peak detection algorithm for LC-MS," *Genomics* 11, Suppl 3: S8.

Zhou, W., Zhu, D., Langdon, A., Li, L., Liao, S., and Tan, L. (2009). "The structure characterization of cellulose xanthogenate derived from the straw of *Eichhornia crassipes*," *Bioresource Technol*. 100, 5366-5369.

Article submitted: June 13th, 2012; Peer review competed: July 11, 2012; Revised version received and accepted: July 10, 2012; Published: September 14, 2012.